



Original Paper

Mechanisms of water layer thickness and ullage height on crude oil boilover: A theoretical model coupling the effects of multiple physical fields

Qi Jing^{a, c}, Cong Yan^{a, c}, Guo-Hua Luan^b, Yun-Tao Li^{a, c, *}, Lai-Bin Zhang^{a, c}, Yue-Yang Li^{a, c}, Xin Li^b, Yun-He Zhang^{a, c}, Xing-Wang Song^{a, c}

^a College of Safety and Ocean Engineering, China University of Petroleum, Beijing, 102249, China

^b CNPC Research Institute of Safety & Environment Technology, Beijing, 102206, China

^c Key Laboratory of Oil and Gas Safety and Emergency Technology Ministry of Emergency Management, Beijing, 102249, China

ARTICLE INFO

Article history:

Received 5 January 2024

Received in revised form

9 June 2024

Accepted 29 August 2024

Available online 30 August 2024

Edited by Jia-Jia Fei and Teng Zhu

Keywords:

Boilover

Ullage height

Water layer thickness

Burning rate

Boilover onset time

Boilover intensity

ABSTRACT

Boilover is one of the most destructive tank fire scenarios. A series of experiments were conducted using eight different depths of oil pans (ranging from internal depths of 4–20 cm) to vary the water layer thickness and ullage height. The results indicate that the water layer effectively cools the sidewalls, reduces the burning rate, inhibits the development of hot zones, and delays the onset of boilover in small and medium-scale experiments. Conversely, the ullage height affects the burning rate, formation of hot zones, intensity of the boilover, and boilover onset time. Utilizing experimental data and thermodynamic analysis, both water layer thickness and fuel layer thickness were considered as variables to predict sidewall temperature at the fuel surface. These results were then introduced into the burning rate prediction model. A prediction model for the boilover onset time was also developed using the water layer thickness as a variable, and a thermodynamic analysis revealed the existence of a limit to the effect of water layer thickness on the boilover onset time. Bubble dynamics was introduced to analyze the boilover process at the oil-water interface, clarifying that the influence of water layer thickness and ullage height on boilover intensity primarily lies in factors such as the degree of superheat at the fuel-water interface. The study's findings hold significant implications for predicting and assessing fire accidents in storage tanks.

© 2024 The Authors. Publishing services by Elsevier B.V. on behalf of KeAi Communications Co. Ltd. This is an open access article under the CC BY-NC-ND license (<http://creativecommons.org/licenses/by-nc-nd/4.0/>).

1. Introduction

Energy serves as the foundation of modern society. Since 1950, when oil emerged as the primary source of global energy consumption, the proliferation of crude oil storage tanks and reservoirs has been relentless (Deng et al., 2021; Jing et al., 2023, 2024; Zhao et al., 2021). For crude oil storage facilities, fire can have a devastating effects (Li et al., 2024). Among various fire accidents, boilover is recognized as a particularly severe scenario due to its potential for rapid escalation. Studies on boilover fires can be categorized into hot zone boilover and thin-layer boilover based on the formation of a hot zone or the initial oil layer thickness, most tank

boil-over fires are hot zone boilover. Hot zone boilover involves the expulsion of water from the storage tank, accompanied by a substantial volume of oil. This sudden release causes a rapid expansion of flames, leading to a dramatic surge in heat radiation. The resulting ignition can potentially ignite adjacent tanks, increasing the scale of the incident (Shaluf and Abdullah, 2011). Over the years, a series of boilover accidents from Whiting, Indiana in 1955 (Ahmadi et al., 2019), to Cangzhou, China in 2021, serves as a somber testament to the gravity of this phenomenon. Therefore, it is necessary to conduct research on the phenomenon of hot zone boilover.

Studies on boilover have been conducted for decades, with Hall (1925) being one of the first to describe the phenomenon. During the combustion of wide boiling range oil, a region of constant temperature known as the hot zone forms inside the oil. The hot zone continuously expands downwards during the combustion

* Corresponding author.

E-mail address: liyt@cup.edu.cn (Y.-T. Li).

process until it reaches the bottom and heats the water, leading to an explosive phase change. The formation and expansion of the hot zone are crucial factors contributing to boilover (Koseki et al., 2006). Burgoyne (1947), Hasegawa (1989), Koseki et al. (1991, 2006), conducted experiments using tanks of different sizes and found that the continuous cycle of light components rising and heavy components sinking with heat during combustion is a significant reason for the continuous formation and expansion of the hot zone. Broeckmann and Schecker (1995) investigated fuel types and thicknesses, finding that bubble generation from lighter component fuels at the hot-cold interface induces strong convection, resulting in a constant temperature and component in the hot zone. Similarly, Tseng et al. (2020) and Wan Kamarudin and Buang (2016) also identified the role of bubble generation in hot zone development. However, Blinov and Khudyakov (1961) conducted small and medium scale experiments suggesting that hot zone growth occurs through heat transfer via the tank wall, and boilover only transpires upon reaching the nucleation boiling temperature. Nakakuki (1997), while cooling the tank with water during the study, observed the hot zone shrinking until it disappears, noting that an increase in tank wall thickness accelerates thermal dissemination. Arai et al. (1990) proposed that significant radiation from the flame heating the fuel layer contributes to hot zone formation. Persson and Lönnermark (2004) conducted experiments and analyses and suggested that three conditions are necessary for boilover to occur: water in the oil, the ability to form a hot zone, and a certain viscosity of the oil.

In addition to the mechanisms of boilover occurrence and hot zone formation and expansion, there has been a significant body of research focused on the combustion process and boilover characteristics. Traditional parameters of pool fire research, such as burning rate, flame height, and radiant heat flow, have also been studied in the context of boilover (Chen and Wei, 2014; Kong et al., 2021). Kong's (Kong et al., 2017) small-scale experiments further classified the process into four stages: development, steady-state combustion, boilover, and decay based on the mass burning rate. Boilover characteristics, such as the rapid increase in flame height, oil spattering, and formation of hot zones, have been extensively studied. Researchers have identified and studied parameters such as boilover intensity, heat wave transfer rate, and spattering range (Ferrero et al., 2007a, b; Garo et al., 1999, 2006; Inamura et al., 1992).

Numerous studies have investigated the mechanism of boilover and explored various parameters affecting its occurrence. For instance, Ping et al. (2018) examined the flame geometry characteristics of boilover under lateral airflow, Ferrero et al. (2007a, b) studied the effect of pool diameter on boilover, and Garo et al. (1996) studied the effect of fuel boiling point in boilover. Tseng et al. (2020) demonstrated the significance of bubble motion at the hot-cold interface in the formation and expansion of the hot zone by introducing a metal grid to increase nucleation points within the fuel layer.

Although significant research has been conducted on the mechanism of boilover, the formation and distribution of hot zones, and the influence of various factors on boilover, little attention has been paid to the thickness of the water layer and the ullage height. The water layer, one of the fundamental components of boilover, significantly influences both the onset of this phenomenon and the formation of hot zones. Moreover, the thickness of the water layer plays a pivotal role in the design of small- and medium-scale experiments and the prediction of real-world boilover incidents. Additionally, ullage height governs limitations on air entrainment and heat transfer from the flame to the fuel surface (Liu et al., 2021; Zhao et al., 2022, 2023), ultimately affecting boilover splatter behavior.

In the present study, a series of small-scale experiments were

conducted to investigate the effects of water layer thickness and ullage height on boilover. Predictive models were established for burning rates and boilover onset times based on heat transfer theory. By examining the key factors affecting boilover intensity, this research aims to provide valuable insights for both predicting and understanding actual boilover incidents. The findings from this study could serve as useful technical references in the field of boilover safety.

2. Experimental setup and models

2.1. Experimental setup

To mitigate potential effects of ambient winds, all experiments were conducted indoors in a hall, with doors and windows kept closed but not sealed during the experiments. The ambient temperature during the experiments was 15.3 °C, with the humidity at approximately 25–10%. The oil utilized in this experiment was crude oil from the Jidong Oil Field, and the relevant parameters of the crude oil are presented in Table 1. Prior to the experiment, the oil was heated in a constant temperature water bath, with an initial oil temperature of 50 °C.

As depicted in Fig. 1, the schematic diagram illustrates the experimental setup. Since most of the accidental tanks are low liquid level and high ullage height situations, eight customized round oil pans made of Q-235 stainless steel were used in the experiments. Each pan has an inner diameter of 10 cm, a sidewall thickness of 3 mm, and a bottom thickness of 3 mm. The internal depths of these pans are 4, 5, 6, 8, 10, 12, 16, and 20 cm. Positioned along the pool axis were nine K-type thermocouples (T1–T9) to monitor temperature changes in the fuel and water layers during combustion. The arrangement of the thermocouples is illustrated in Fig. 2, with a 1 cm interval between T2 and T3 and a 0.5 cm interval between the remaining thermocouples. These thermocouples, with a diameter of 1 mm, facilitated sampling at a rate of twice per second. An electronic balance, with a maximum load of 40 kg and an accuracy of 0.1 g, was utilized to measure oil mass variations during the experiment. Positioned beneath the oil pan, a fire barrier shielded the balance from heat and spatter products generated during combustion. Furthermore, a 30-frame camera was strategically placed within the room to capture and record changes in the flame pattern as well as changes in the audio signal.

The objective of this study is to investigate the influence of water layer thickness and ullage height on boilover. Therefore, the primary variables of interest in this investigation are water layer thickness and ullage height. To gain deeper insights into the impact of water layer thickness (H_w) on boilover, combustion tests were conducted without a water layer, utilizing two different initial fuel layer thicknesses (H_0). Throughout all experiments, the pool diameter remained constant. The specific experimental conditions are depicted in Table 2.

In specific scenarios, particular attention was given to two conditions: (1) in the absence of a water layer, where the T1 thermocouple was positioned 5 mm above the bottom of the oil pan, and (2) when the water layer had a thickness of 1 cm, where the T2 thermocouple was situated at the oil–water interface. For all other working conditions, the T3 thermocouple was placed at the oil–water interface.

Table 1
The characteristics of Jidong crude oil.

Water content	Viscosity	Density	Melting point	Sulfur content
0.26%	32.29 mPa s	0.876 g/cm ³	28 °C	0.212

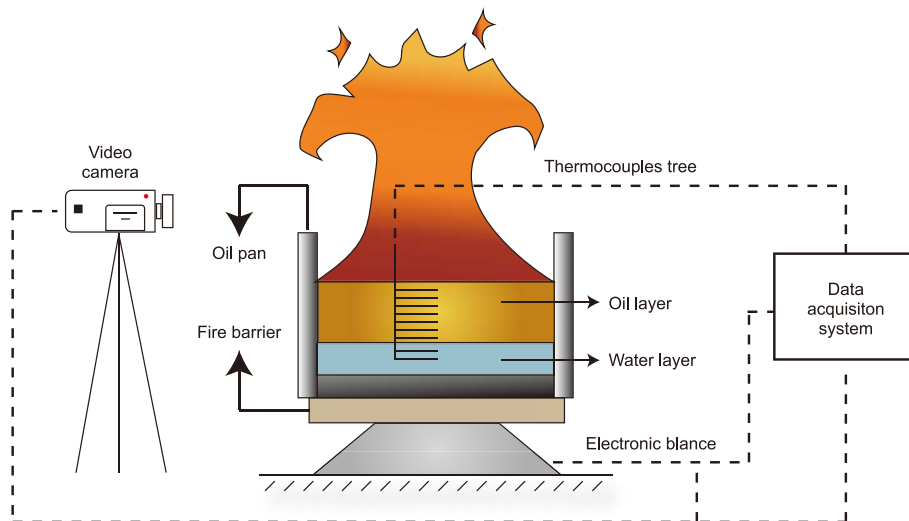


Fig. 1. Schematic of experimental setup.

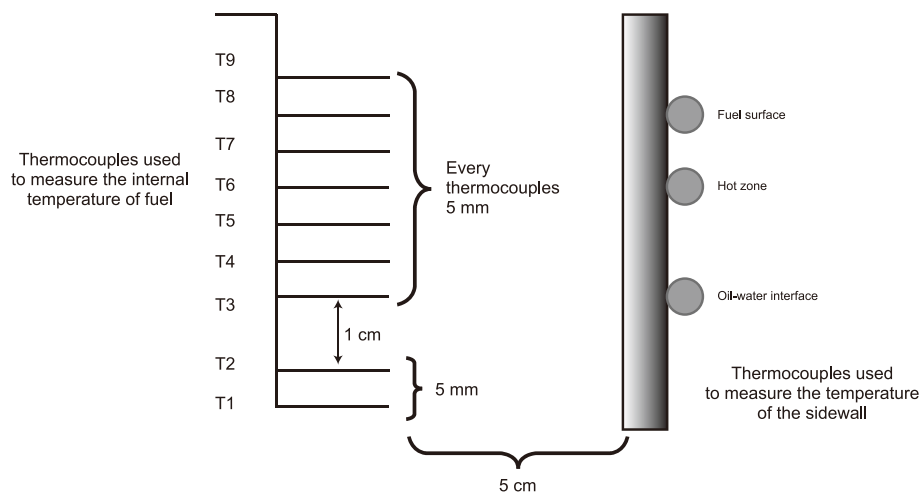


Fig. 2. Schematic representation of the thermocouple tree and the thermocouple employed for temperature measurement.

Table 2
The specific experimental conditions of boilover.

Initial fuel thickness, cm	Pool diameter, cm	Ullage height, cm	Water layer thickness, cm
3	10	1	0, 1, 2, 4, 6, 8
5	10	1	0, 2, 4, 6, 8, 10, 14
5	10	1, 3, 5, 9, 13	2

2.2. Heat transfer models

To gain a better understanding of the combustion behavior specific to the phenomenon of boilover, the primary heat transfer mechanics of the combustion process are analyzed, as illustrated in Fig. 3, primarily adapted from Nakakuki’s study (Nakakuki, 1997). As depicted in Fig. 3, along the y-axis direction, the interior of the entire oil pan can be divided into four parts: the boiling layer, hot zone, cold zone and water layer.

In general, the mass burning rate essentially represents the gasification rate. The burning rate of a pool fire is determined by the energy required to evaporate the fuel versus the net heat flux transferred to the fuel surface, as shown in Eq. (1):

$$\dot{m}'' = \frac{\dot{q}_f'' - \dot{q}_l''}{L_v + \int C_p dt} = \frac{\dot{q}_f'' - \dot{q}_l''}{\Delta H_g} \tag{1}$$

In Eq. (1), the parameters \dot{q}_f'' and \dot{q}_l'' represent the heat input to the fuel surface and the heat loss from the fuel, respectively. The term " $\Delta H_g = L_v + \int C_p dt$ " denotes the heat required for fuel gasification, while L_v signifies the energy needed for fuel evaporation. Additionally, C_p represents the sensible energy required to raise the fuel temperature from its initial state to the temperature at which it evaporates. Furthermore, Fig. 3 illustrates a schematic diagram of the heat transfer inside the liquid and at the tank wall, which can be

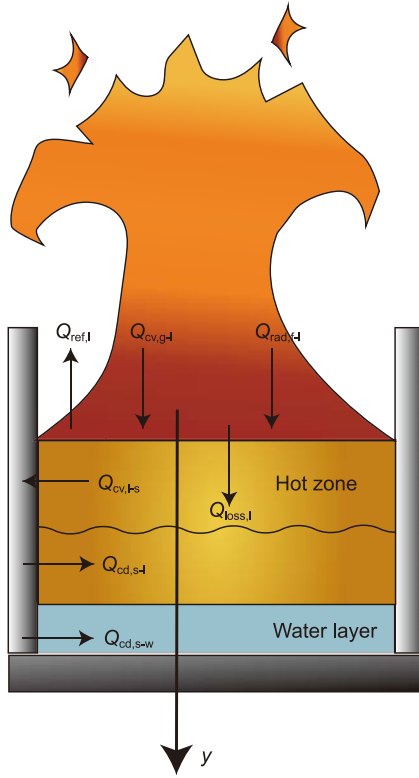


Fig. 3. Schematic representation of the primary heat transfer mechanics for the fuel and the sidewall.

combined with Eq. (1) to obtain a more refined heat balance extrapolation:

$$\dot{m}'' \Delta H_g = Q_{\text{rad},f-l} + Q_{\text{cond},s-lb} + Q_{\text{conv},g-l} - Q_{\text{loss},l} - Q_{\text{ref},l} \quad (2)$$

In Eq. (2), the left side of the equation represents the heat absorbed by the surface of the liquid, $Q_{\text{rad},f-l}$ is the radiation heat from the flame, $Q_{\text{cond},s-lb}$ is the conduction heat from the walls of the tank, $Q_{\text{conv},g-l}$ is the convection heat from the evaporating gases, $Q_{\text{ref},l}$ is the heat reflected from the surface of the liquid, $Q_{\text{loss},l}$ is the heat loss from the surface of the fuel to the deeper layers of the fuel.

The radiative heat from the flame to the fuel surface is given by Chatris et al. (2001), Ditch et al. (2013), Karataş et al. (2013):

$$Q_{\text{rad},f-l} = \sigma F (T_f^4 - T_1^4) [1 - \exp(-\kappa D)] \quad (3)$$

where σ corresponds to the Stefan-Boltzmann constant, F represents the geometric coefficient of the liquid relative to the flame, T_f denotes the flame temperature, while T_1 represents the fuel surface temperature, and κ is the extinction coefficient, D denotes the pool diameter.

The conductive heat feedback from the tank wall to the fuel surface is given as Vali et al. (2015):

$$Q_{\text{cond},s-l} = \pi D L h_{cd} (T_s - T_1) \quad (4)$$

where L is the length of the boiling layer (Vali et al., 2015; Zhao et al., 2018), h_{cd} is the conduction coefficient, T_s corresponds to the temperature of the side wall at the fuel surface.

The convective heat feedback between the fuel vapor and the fuel surface can be obtained through the stagnant layer theory and

is expressed as follows (Quintiere, 2006; Vali et al., 2014):

$$Q_{\text{conv},g-l} = A h_{cv} \left(\frac{\ln(1+B)}{B} \right) (T_g - T_1) \quad (5)$$

where h_{cv} is the convection coefficient, B is the Spalding number, T_g is the temperature of the fuel vapor.

As depicted in Fig. 3, in addition to heat transfer for the fuel surface, heat transfer for the sidewalls and the internal liquid also occurs underneath. $Q_{cv,l-s}$ represents the heat transfer in the hot zone from the hot zone to the sidewalls during combustion with a water layer, $Q_{cd,s-lc}$ represents the heat transfer in the cold zone from the sidewalls to the cold zone, and $Q_{cd,s-w}$ represents the heat transfer in the water layer from the sidewalls to the water layer. It's essential to emphasize that when the hot zone extends to the oil-water interface, the sidewall temperature is lower than the temperature at the oil-water interface.

Where Eq. (2) will be utilized to analyze and discuss changes in burning rate, variations in $Q_{cv,l-s}$, $Q_{cd,s-lc}$ and $Q_{cd,s-w}$ have a notable impact on alterations in the internal temperature of the fuel during the combustion process. Further elaboration on these effects will be provided later in the discussion.

3. Results and analysis

3.1. Mass burning rate

The mass burning rate plays a pivotal role in the combustion process, representing the rate of evaporation from the fuel surface. It serves as a defining factor for both pool fire characteristics and boilover characteristics. Direct measurement of the burning rate is hindered by the presence of the flame. In this experiment, an electronic balance was employed to measure mass changes, and a previously established conversion factor was used to convert the mass loss rate into the mass burning rate. The change in mass burning rate during the combustion process can be categorized into four stages (Chen et al., 2023; Kong et al., 2017): (1) Growth stage, (2) Quasi-steady stage, (3) Boilover stage, and (4) Decay stage. As illustrated in Fig. 4, the evolution of mass and mass burning rate under typical operating conditions is depicted.

As shown in Figs. 4 and 5, during the boilover stage there is a sharp increase in flame height along with a surge in mass burning rate. This surge can be attributed to the expulsion of oil droplets

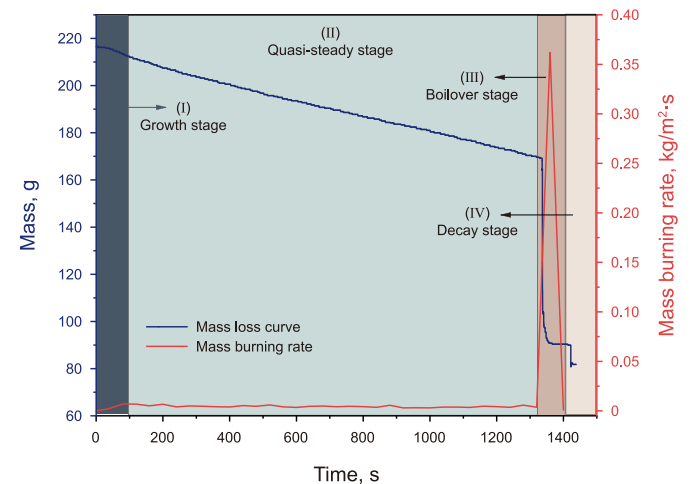


Fig. 4. Temporal evolution of burning rate and mass for a set of typical operating conditions ($H_0 = 3$ cm, $H_w = 5$ cm).

caused by the presence of water. It is worth noting that, according to Ferro et al.'s (Ferrero et al., 2006) study, the evaporation of water is negligible compared to the amount of oil droplets expelled. However, in this process, the expelled oil droplets are considered as consumed by combustion, resulting in a certain discrepancy between the calculated and actual mass burning rates.

Hottel (1959) conducted research on the enthalpy balance and the scale of the fuel surface, providing a semi-quantitative analysis of heat transfer from the fuel surface, this analysis suggests that the term " q_1'' " in Eq. (1) can be approximated to zero. The mass burning rate is primarily influenced by the scale effect, particularly in the mesoscale range ($0.03 \text{ m} < D < 1.0 \text{ m}$), where the radiation term plays a significant role, as shown in Eq. (6) (Drysdale, 2011):

$$\dot{m}'' \approx \frac{\sigma F (T_f^4 - T_1^4)}{\Delta H_g} [1 - \exp(-\kappa D)] = \dot{m}_{\max}'' [1 - \exp(-\kappa D)] \tag{6}$$

As depicted in Fig. 6, the variation in burning rate during the quasi-steady state period for different water layer thicknesses is apparent. There's a substantial reduction in burning rate with increasing water layer thickness, considering it as the sole variable. This experimental finding deviates from Hottel's semi-quantitative analysis.

Through the thermodynamic analysis combined with Eqs. (1)–(5), it can be found that variations in burning rate are primarily governed by the heat balance of the fuel surface. The boiling point of the fuel and the flame temperature in both radiation and convection terms are inherent to the fuel composition, which means that the radiation term and the convection term are almost unaffected by the thickness of the water layer. Consequently, the change of the thickness of the water layer is mainly related to the heat conduction term. Furthermore, sidewall temperatures were measured throughout the experiment. Along the y-axis direction as depicted in Fig. 3, we observed a negative correlation between sidewall temperature and its distance from the fuel surface, the sidewall temperature decreased with increasing water layer thickness (H_W). Hence, we conclude that the water layer provides a cooling effect on the sidewalls, illustrated as $Q_{cd,s-w}$ in Fig. 3. This cooling effect becomes more pronounced with a thicker water

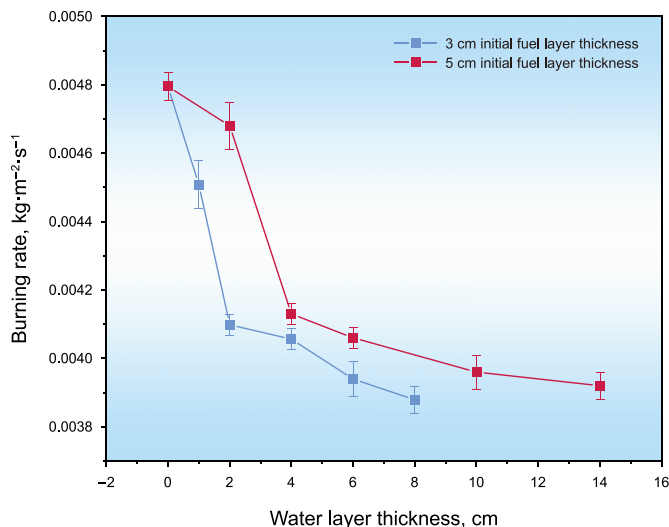


Fig. 6. Steady burning rate comparison of the different water layer thicknesses for different initial fuel layer thicknesses.

layer. It's worth noting that the influence of the cooling effect on the burning rate is also affected by the initial fuel layer thickness (H_0), which can be explained by heat transfer. H_0 represents the distance from the fuel surface to the water layer, and the larger H_0 is, the smaller the effect on T_s .

In particular, it should be emphasized that there is a limit to the water cooling effect on T_s . When the water layer thickness exceeds a certain value, T_s will reach a minimum temperature, which does not change further, and the minimum value of T_s is positively correlated with H_0 . Therefore, the connection between T_s , H_0 , and H_W is established by fitting, and the results are shown in Fig. 7 and Eq. (7) and Eq. (8):

$$T_s = 45.57 \exp(-H_W/3) + 349.6 \tag{7}$$

$$T_s = 45.57 \exp(-H_W/5) + 353.94 \tag{8}$$

If the fitted equations are incorporated into Eqs. (2)–(6), we

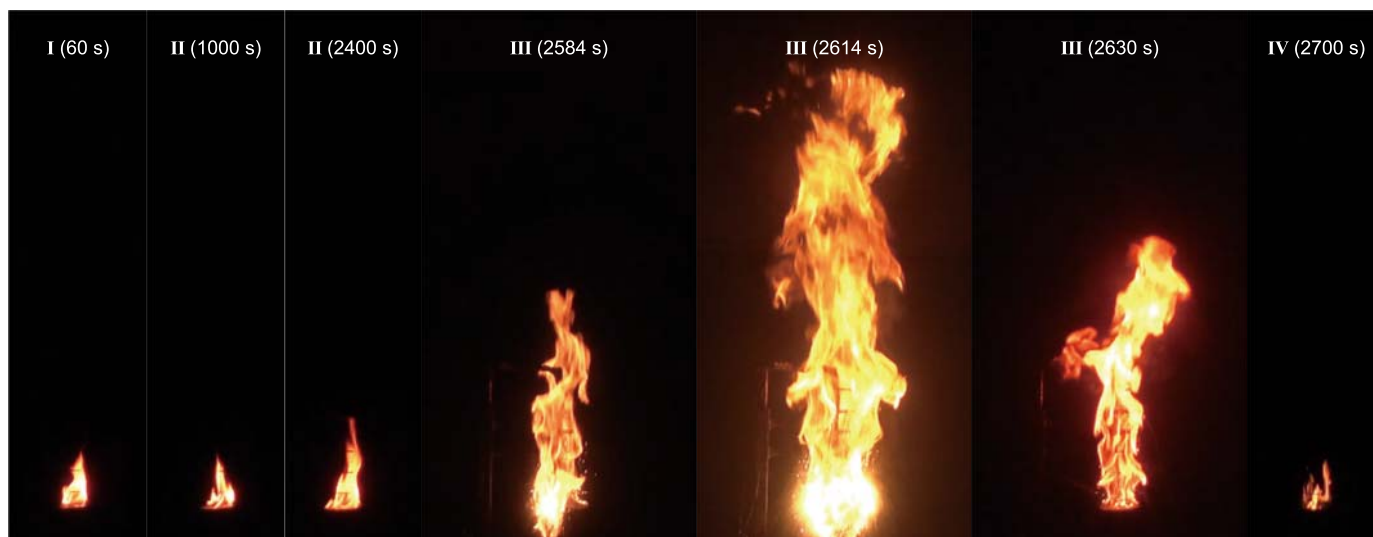


Fig. 5. Evolution of the flame during the boilover fire ($H_0 = 5 \text{ cm}$, $H_w = 2 \text{ cm}$).

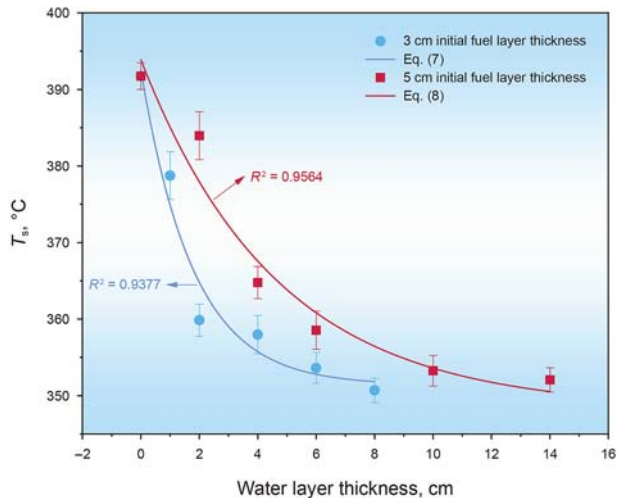


Fig. 7. Comparison of the T_s of the fuel surface for different water layer thicknesses and different initial fuel layer thicknesses, along with the fitting of Eq. (7) and Eq. (8).

derived prediction equations for the mass burning rate during the quasi-steady state period with water thickness as a determining factor, as presented in the following Eq. (9):

$$\begin{aligned} \dot{m}'' &\approx \frac{\sigma F (T_f^4 - T_1^4)}{\Delta H_g} [1 - \exp(-\kappa D)] + \frac{ALh_{cd}(T_s - T_1)}{\Delta H_g} = \\ \dot{m}''_{\max} [1 - \exp(-\kappa D)] &+ \frac{ALh_{cd}}{\Delta H_g} [45.57 \exp(-H_W/H_0) + T_{s,\min} - T_1] \end{aligned} \quad (9)$$

where H_W represents the water layer thickness, H_0 represents the initial fuel layer thickness, and $T_{s,\min}$ represents the minimum value of the sidewall temperature at the fuel surface location as the water layer thickness approaches its limit. It's important to highlight that the analysis above is based on small-scale boilover fire experiments. In larger-scale fire scenarios, thermal radiation becomes the primary heat transfer mechanism, and the decrease in conduction heat induced by water-cooling effect may have a negligible effect on the burning rate.

As depicted in Fig. 8, a comparison of burning rates at varying ullage heights reveals a clear trend: as the ullage height increases, the burning rate initially rises and subsequently declines. An experiment with an ullage height of 13 cm was conducted in this study, however, it's important to highlight that the flame self-extinguished within a few seconds from the experiment's commencement. As shown in Fig. 4, altering the ullage height results in an expanded heating surface for both radiation and convection along the tank wall. This, in turn, elevates the sidewall temperature, consequently reflecting an increase in the burning rate. However, as the ullage height continues to rise, it becomes increasingly susceptible to the influence of air entrainment, as observed in the experimental data presented in Fig. 8, leading to a decrease in the rate of combustion until self-extinguishing.

3.2. Temperature variation within fuel

During combustion, wide-boiling range oils such as crude oil and diesel oil develop an isothermal layer beneath the fuel surface, commonly referred to as the "hot zone", as depicted in Fig. 9. As combustion progresses, the temperature within this zone steadily rises, consistent with findings from prior research (Hasegawa,

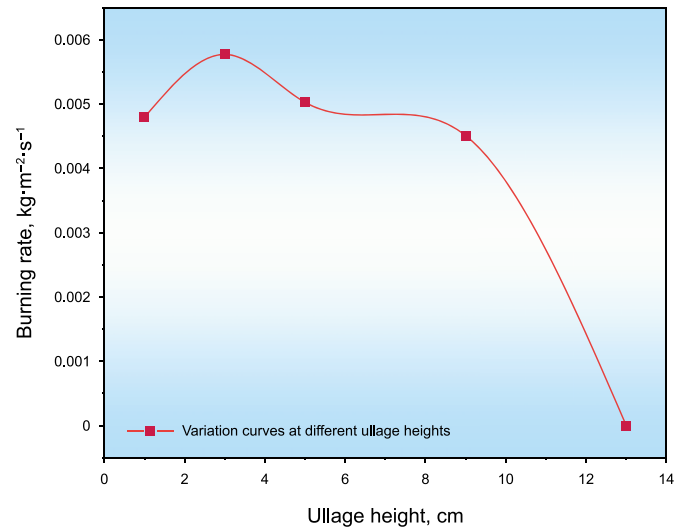


Fig. 8. Comparison of steady burning rates for different ullage heights.

1989; Koseki, 1993; Koseki et al., 1991).

The temperature of the hot zone, a critical aspect, is largely governed by the oil type, consistent with the principles outlined in (Nakakuki, 1997). Distinct variations exist in the hot zone temperature across different oil types. In our study, employing Jidong crude oil, the initial hot zone temperature registers at 170 ± 5 °C during the zone's inception. As time elapses, the temperature escalates, eventually reaching 200 ± 5 °C.

In this study, we have identified a phenomenon that deviates from the conventional formation of a thermal zone. As illustrated in Fig. 9, this phenomenon involves the stratification of the thermal zone. Specifically, the thermocouple reaches a stable temperature after a certain period, displaying minimal fluctuations over time. However, intriguingly, a discernible temperature gradient forms along the axial direction. Notably, the temperature within the water layer (located closer to the axis) registers lower than the typical temperature of the thermal zone. This observation adds a new layer of complexity to our understanding of hot zone formation.

In Fig. 10(a), with a 1 cm water layer, a conventional hot zone forms near the fuel surface until boilover occurs. However, in Fig. 10(b), an initial hot zone is established, but delamination sets in after approximately 1000 s of combustion. As depicted in Fig. 10(c)–(e), a standard hot zone fails to develop throughout the combustion process.

Furthermore, it's important to highlight that the presence of this temperature gradient differs from the distribution of fuel within individual combustion instances. While a solitary combustion event follows an exponential fuel distribution pattern, the temperature distribution observed in the experiment portrays a linear configuration. Refer to Fig. 11 for a visual representation of this scenario.

In Fig. 11, T_b denotes boiling point of fuel, T_{hz} represents hot zone temperature, and T_0 signifies ambient temperature. Hasegawa (1989) and Boreckman and Schecker's (1995) theory posits that the genesis and evolution of the hot zone emanate from discrepancies in boiling points among oil components. Components with lower boiling points generate bubbles upon reaching their boiling points, precipitating abrupt volume fluctuations, trigger the ascent of bubbles. This oscillatory behavior, observed prior to thermocouples entering the hot zone (as seen in Figs. 9 and 10). Subsequently, these bubbles give rise to vigorous convection currents that homogenize the hot oil zone's temperature and components.

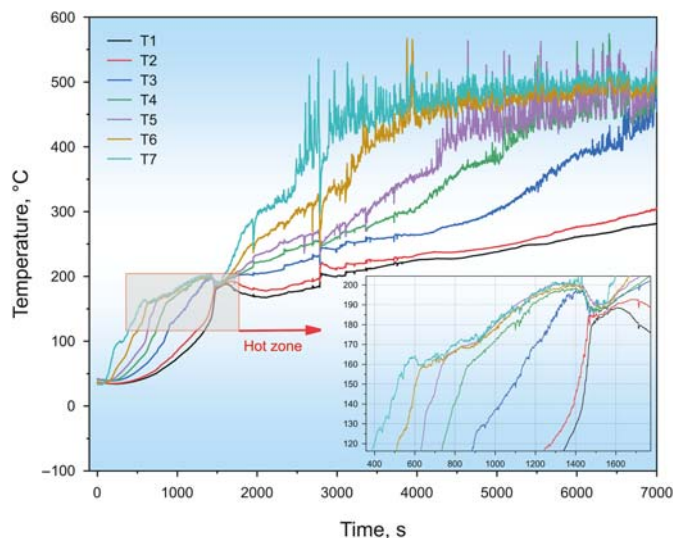


Fig. 9. A typical set of internal fuel temperature variations and hot zone formation in the absence of a water layer.

This convection-driven process underpins the hot zone's formation and expansion. However, this theory inadequately explains the emergence of non-standard hot zones with stratified layers displaying conspicuous temperature gradients, as previously noted.

Nakakuki (1997) investigated heat transfer within small and medium-scale liquid fires with hot zone formation, utilizing containers varying in material and wall thickness. The study revealed distinct hot zone formation and burning rates influenced by differing thermal conductivities of containers. Similarly, in one of Blinov and Khudyakov's (1961) reports, water cooling of a burner with a forming hot zone led to a gradual reduction in the hot zone until its disappearance.

Previous studies have explored the impact of sidewalls on hot zone formation and development. When analyzed alongside Fig. 3, it becomes apparent that the earlier-mentioned water-cooling effect is responsible for this phenomenon. An increase in the water layer's thickness intensifies the water-cooling effect, resulting in a reduction of sidewall temperature. This decrease in sidewall temperature causes the heat from the hot zone not only to propagate downward but also to transfer to the sidewall.

During this study, temperature measurements were taken at horizontal positions corresponding to one-half of the distance from the axial line and close to the tank wall, using T5 thermocouple. The results of these measurements reveal a gradual temperature decrease from the axial line towards the outer edge.

Hence, the formation of the non-standard hot zone in Fig. 9 can be attributed to a combination of axial convection and radial heat transfer. Axial convection plays a pivotal role in maintaining temperature stability over an extended duration and drives the downward expansion of the hot zone. Simultaneously, radial heat transfer results in lower edge temperatures compared to the center, ultimately giving rise to the non-standard hot zone.

The hot zone also exhibits some degree of change under the influence of the ullage height factor, as evidenced by an increase in the maximum temperature of the hot zone, which aligns with the previous analysis.

3.3. Boilover onset time

Boilover occurs when energy accumulates at the bottom of the oil product, leading to the formation of bubbles upon continuous

heating. These bubbles rupture during their ascent, causing oil droplets to splatter. This process generates distinctive noise, which, according to the research by Hua et al. (1998), can serve as an indicator of boilover.

As depicted in Fig. 12, changes in the acoustic spectrum occur before and during boilover. It's evident that boilover commences around the 2400 s mark. In addition to using audio signals to identify boilover, one can also observe an instantaneous increase in burning rate (as seen in Fig. 4) or a sudden surge in flame height. Nevertheless, employing audio signal analysis stands out as a simpler and more accurate method for detection (Hua et al., 1998).

As illustrated in Fig. 13, variations in boilover onset time are observed across different water layer thicknesses and initial fuel layer thicknesses. When analyzing the impact of water layer thickness as the primary variable, a discernible trend emerges: with increasing water layer thickness, there is a delay in the occurrence of boilover until it approaches a limiting value. This suggests that there is a maximum effect of water layer thickness on boilover onset time. This relationship can be precisely expressed through the following Eq. (10):

$$t_b = t_{b,\max}[1 - \exp(-h_w)] \quad (10)$$

Where t_b is the boilover onset time, $t_{b,\max}$ is the limit value of the boilover onset time when the thickness of the water layer is used as a single variable, h_w is the thickness of the water layer, and as per Eq. (10), the limit value of the boilover onset time is 1347 s for an initial fuel layer thickness of 3 cm. Fig. 13 highlights a significant trend: as the initial fuel layer thickness increases, the boilover onset time also increases. This observation aligns with Ferro's findings, which indicate a linear relationship between boiling time and the initial fuel layer thickness.

This phenomenon can be elucidated through the mechanism of boilover. In scenarios where hot zones form, heat transfer at the oil-water interface primarily occurs through conduction. With a greater initial fuel layer thickness, more time is required for the bottom of the oil-water interface to reach the boiling temperature of the water. Moreover, due to the oil-water interface being immersed in water and lacking the necessary conditions for bubble formation, the temperature at the interface is typically superheated, usually by around 20 °C.

The influence of water layer thickness on boilover onset time arises from two main factors. Firstly, the cooling effect of water leads to a reduction in the burning rate and promotes thermal zone stratification. This results in a slower expansion of the hot zone and a decrease in the temperature near the bottom of the hot zone.

Secondly, the cooling effect of water affects sidewall temperatures, which, in turn, has implications for the oil-water interface. Specifically, the sidewall temperature is lower than that of the interface, causing it to take a longer time to reach the superheating temperature at the oil-water interface. In our experiments, sidewall temperatures at the oil-water interface were measured, revealing that during boilover, the sidewall temperature was approximately 80 °C, while the central temperature at the oil-water interface had already reached approximately 120 °C.

As illustrated in Fig. 14, the impact of ullage height on boilover onset time is evident, showcasing a significant influence when the water layer thickness remains constant. Notably, as the ullage height increases, the boilover onset time initially decreases before increasing again, a phenomenon easily explained. As discussed in Section 3.1, the burning rate experiences an initial surge followed by a decline until self-extinguishing with increasing ullage height. This surge in the burning rate accelerates the transfer of heat to the water layer, resulting in a reduction in boilover onset time. Conversely, a continued increase in ullage height subsequently

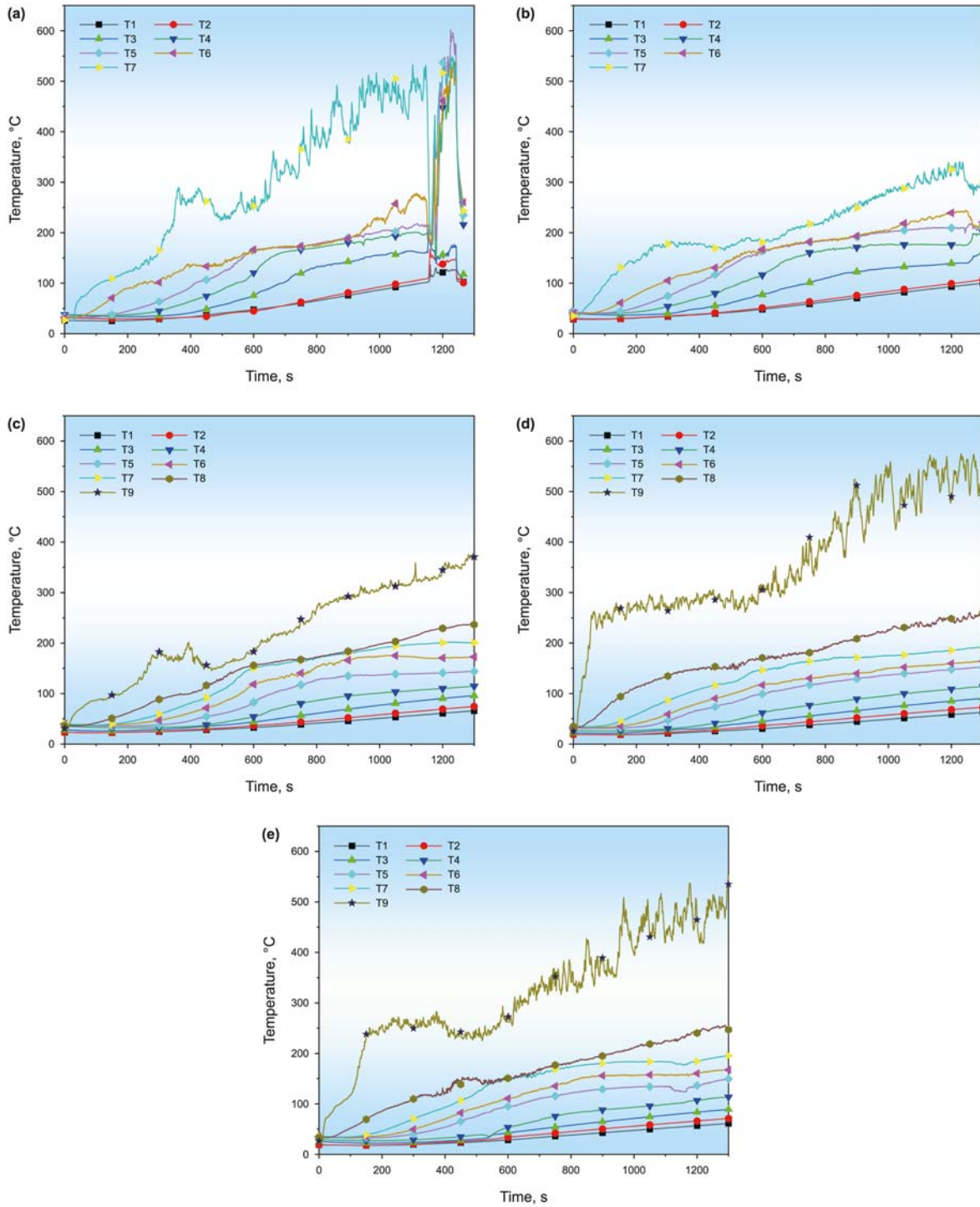


Fig. 10. Variation of internal temperature of fuels at different water layer thicknesses and thermal zone stratification when $H_0 = 3$ cm (From (a)–(e) denote water layer thicknesses of 1, 2, 4, 6 and 8 cm, respectively.)

decreases the burning rate, thereby prolonging the boilover onset time.

3.4. Boilover intensity

Boilover intensity, a crucial parameter, assesses the severity of boiling. Initially, Koseki et al. (1991) quantified it as the ratio of burning rates during the quasi-steady state period and the boilover period. Ferrero refined this approach, expressing it as the

percentage increase or decrease in burning rate during boilover relative to the quasi-steady state period. This modification is presented in Eq. (11) and Eq. (12) below (Ferrero et al., 2007a, b):

$$I_{b,av} = \frac{\dot{m}_{b,av} - \dot{m}_s}{\dot{m}_s} \times 100 \tag{11}$$

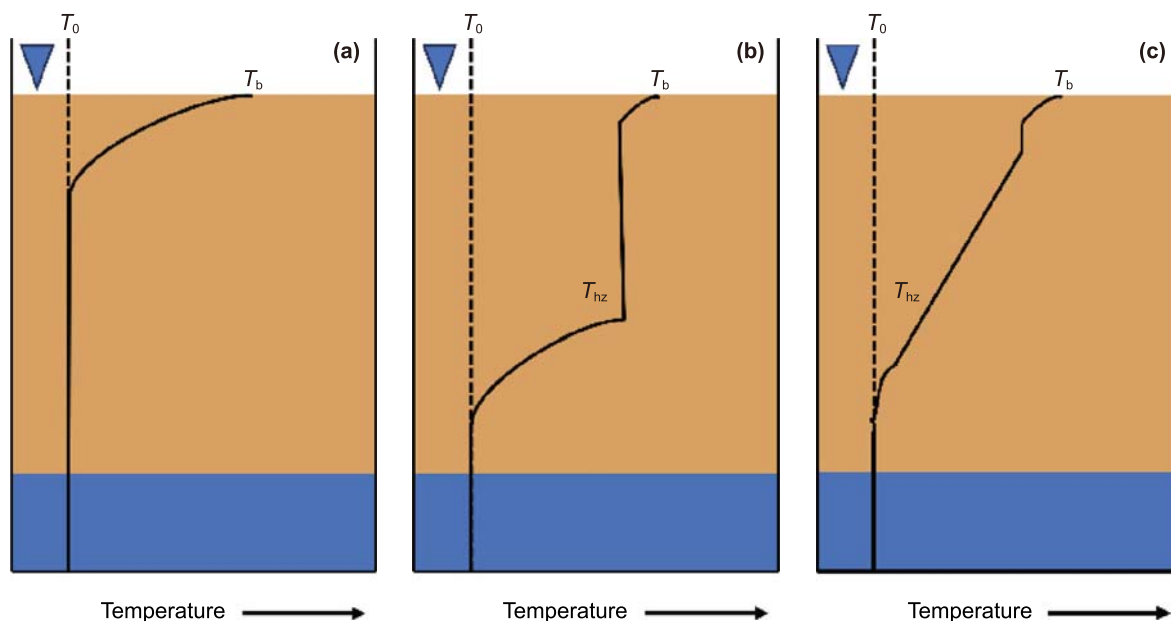


Fig. 11. Internal temperature profiles of the combustion process of different fuels are illustrated from left to right: a single fuel, a fuel with hot zone formation, and a fuel with water-cooling leading to thermal zone stratification.

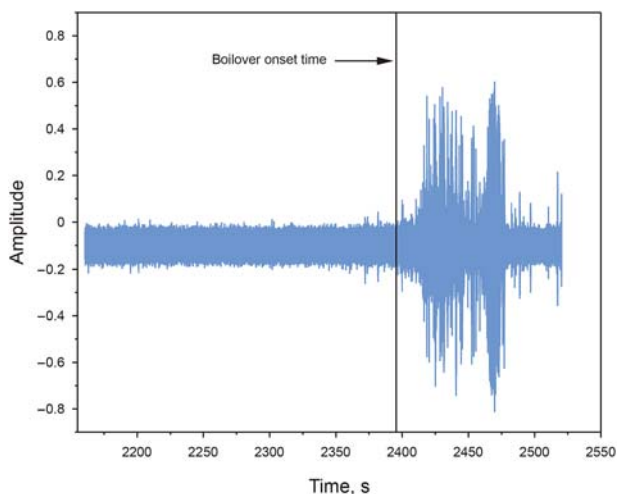


Fig. 12. Determination of boilover onset time by audio signal analysis.

$$I_{b,max} = \frac{\dot{m}_{b,max} - \dot{m}_s}{\dot{m}_s} \times 100 \quad (12)$$

where $I_{b,av}$ signifies average boilover intensity, $\dot{m}_{b,av}$ is the average mass burning rate during boilover, $I_{b,max}$ denotes the maximum boilover intensity, and $\dot{m}_{b,max}$ represents the maximum mass burning rate of a single splash.

In this experiment, increasing the water thickness reduced the boilover duration, rendering average boilover intensity less effective for characterizing boilover intensity. Conversely, the maximum boilover intensity captures the peak moment in a single boilover event, offering a clearer indication of water layer thickness. This metric aptly reveals the influence of water layer thickness and ullage height on boilover intensity. As shown in Fig. 15, the maximum boilover intensity varies under different water layer thicknesses.

The maximum boilover intensity, a key parameter, exhibits

intriguing behavior in response to varying water layer thicknesses. Upon analyzing the data, a noteworthy pattern emerges. As the initial fuel layer thickness increases, the maximum boilover intensity tends to rise, consistent with earlier research findings. The effect of the initial fuel layer thickness on $I_{b,max}$ is also well understood. At the same water layer thickness, the difference in burning rate between different initial fuel layer thicknesses is not very large. However, the larger the fuel layer thickness, the later the boilover occurs. Yet, just before the boilover, a larger fuel layer thickness results in more fuel remaining, which can be encapsulated in the bubbles formed by the phase transition of the water, as depicted in Fig. 15.

In Fig. 15, it can also be observed that $I_{b,max}$ tends to increase and then decrease when the water layer thickness is used as a single variable, and it can be predicted that there exists a limiting value of $I_{b,max}$ when the water layer thickness is used as a single variable, based on the previous analysis combined with the trend in Fig. 15.

To unravel this phenomenon, we delve into the mechanisms of boilover. Boilover necessitates boiling of the water layer, which, in turn, involves two distinct processes: homogeneous nucleation and heterogeneous nucleation. While the hot zone extends to the oil-water interface, nucleation conditions for boiling aren't met due to excessive immersion. Research by Apfel (1971) and Jarvis et al. (1975), alongside our own experimental results, suggest that boilover predominantly occurs through heterogeneous nucleation. In this process, nucleation conditions are facilitated by particles generated during combustion (Laboureur et al., 2013). We can represent homogeneous and non-homogeneous nucleation as follows (Reed-Hill et al., 1973):

$$\Delta G_c^{het} = \Delta G_c^{hom} \frac{(2 - \cos \theta + \cos^3 \theta)}{4} \quad (13)$$

where ΔG_c^{het} represents the energy required for heterogeneous nucleation, ΔG_c^{hom} represents the energy required for homogeneous nucleation, θ represents the contact angle. Laboureur's high-speed camera records during boilover reveal that bubbles formed at the oil-water interface grow into smaller bubbles. After some time,

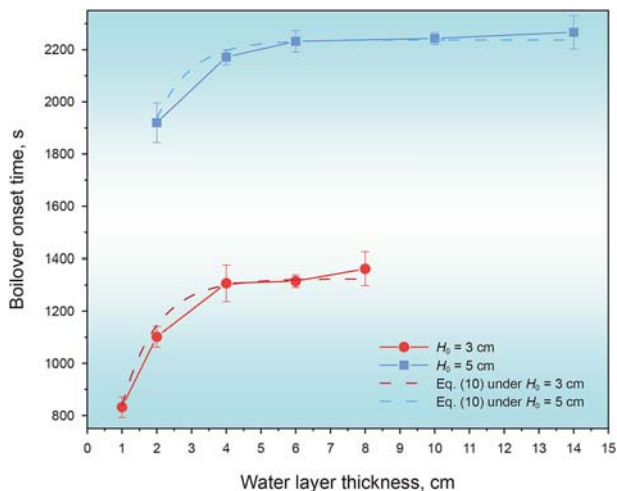


Fig. 13. Comparison of boilover onset times across different water layer thicknesses for various initial fuel layer thicknesses, along with the fitting of Eq. (10).

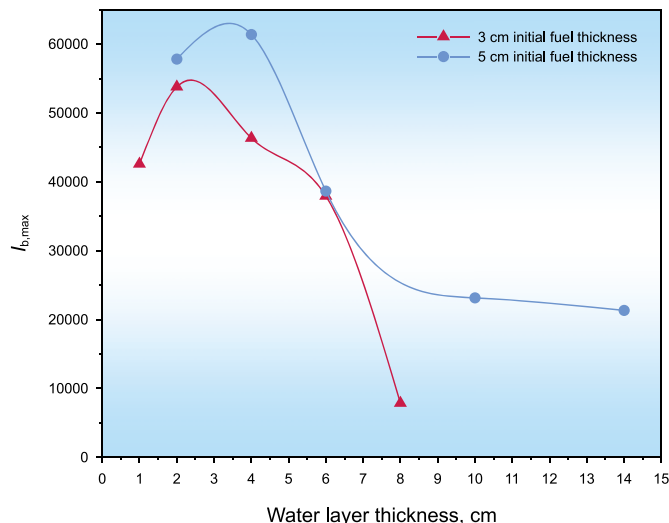


Fig. 15. $I_{b,max}$ comparison of the different water layer thicknesses for different initial fuel layer thicknesses.

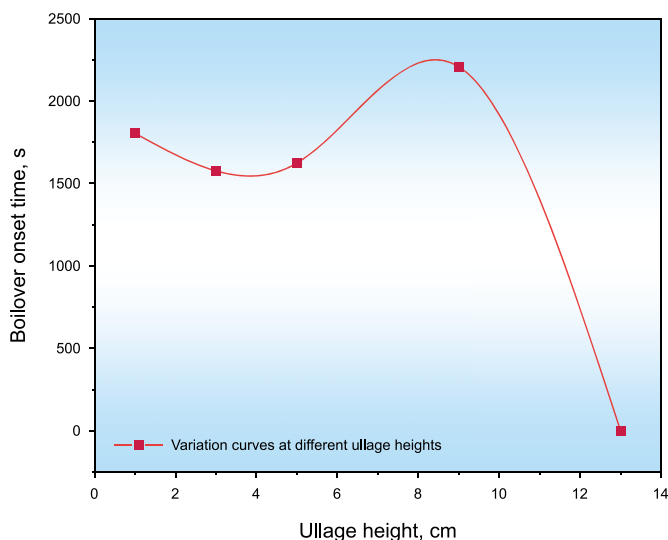


Fig. 14. Comparison of boilover onset times at different ullage height.

these bubbles depart from the interface, stirring the oil and leading to boilover. The relationship between bubble growth rate and temperature is captured in the equation below (Reed-Hill et al., 1973):

$$\nu \propto \left(e^{-\Delta ga/\kappa T} \right) \quad (14)$$

where ν is the rate of bubble growth rate, Δga is energy barrier, κ is Boltzmann constant, T is the temperature. It can therefore be concluded that the decrease in maximum boiling intensity is due to the presence of water cooling. The increase in the thickness of the water layer leads to the deepening of the water cooling effect, resulting in a decrease in the burning rate. The time required for particle generation and settlement is longer, prolonging the time for heat to reach the oil-water interface. Additionally, the temperature of the fuel layer above the oil-water interface decreases due to the water cooling effect. Simultaneously, the lower temperature of the sidewalls, caused by water cooling, leads to heat loss from the interface to the sidewalls, further reducing the interface temperature compared to the expected temperature. Consequently, the

boiling time is delayed, affecting the nucleation rate and nucleation size. This delay in boiling time significantly reduces the maximum boiling intensity. As a result, boilover occurs later, and the nucleation rate and nucleation size are affected, leading to a significant decrease in the maximum boilover intensity, as shown in Figs. 13 and 15.

Building upon the discussed theory, it becomes evident that the number of generated bubbles also influences boilover intensity. This relationship is aptly illustrated by the initial growth trend seen in Fig. 15. Boilover intensity can be seen as a multifaceted function, influenced by various factors, including the duration of boiling, the quantity of flue gas produced, the temperature at the oil-water interface, and the remaining fuel mass before boilover. During the initial phase of water layer thickness growth, although the critical bubble diameter decreases, the extended boilover onset time results in more settling particles, leading to an increased bubble generation. This dynamic is clearly depicted in the initial growth phase of Fig. 15.

4. Conclusion

A series of experiments were conducted to investigate the effects of water layer thickness and ullage height on boilover. Subsequently, a burning rate prediction model and a boilover onset time model were constructed through thermodynamic analysis to elucidate the impacts of water layer thickness on boilover. Additionally, bubble dynamics and superheat theory were introduced to examine the intensity of boilover. The main findings are summarized as follows:

- (1) The thickness of the water layer induces a water cooling effect on the sidewall, which consequently impacts boilover. This effect amplifies with increasing water layer thickness. Through thermodynamic analysis combined with a multi-parameter prediction model of sidewall T_s , adjustments were made to the burning rate model. Simultaneously, utilizing water layer thickness as a single variable, a prediction model for boiling time was developed. This predictive model facilitated the determination of the limit value of the burning rate and boilover onset time.
- (2) The ullage height serves a dual function, acting as a constraint on air entrainment while simultaneously

enhancing sidewall heat transfer through the expansion of the convection zone. These roles are interdependent and influenced by the ullage height itself. In scenarios where the ullage height is small, sidewall heat takes precedence, resulting in an increase in the burning rate and an earlier onset of boilover. Conversely, as the ullage height increases, the limitation imposed by air entrainment becomes dominant, leading to a decrease in the burning rate and a delayed onset of boilover.

- (3) Boilover intensity is determined by the superheat of the fuel-water interface. The higher the superheat, the higher the boilover intensity. The thickness of the water layer leads to a reduction in the boilover intensity, precisely through the effect of water cooling leading to a reduction in the superheat of the fuel-water interface, which is caused by the particles provided by prolonged combustion at a lower degree of superheat. Since the bubbles are expanding as they rise, the increase in the thickness of the fuel layer leads to an increase in the boilover intensity as it is able to carry more fuel splash out during the expansion process.

CRediT authorship contribution statement

Qi Jing: Writing – review & editing, Supervision, Methodology. **Cong Yan:** Methodology, Data curation. **Guo-Hua Luan:** Investigation, Data curation. **Yun-Tao Li:** Writing – original draft, Funding acquisition. **Lai-Bin Zhang:** Supervision, Investigation. **Yue-Yang Li:** Investigation, Conceptualization. **Xin Li:** Investigation, Data curation. **Yun-He Zhang:** Supervision, Investigation. **Xing-Wang Song:** Supervision, Data curation.

Declaration of competing interest

The authors declare that they have no known competing financial interests or personal relationships that could have appeared to influence the work reported in this paper.

Acknowledgment

This article was supported by the National Natural Science Foundation of China (Project Approval Number: 52374253), China National Petroleum Corporation Scientific Research and Technological Development Programs (Project Approval Number: 2022DJ6808), China Postdoctoral Innovative Talent Support Program (Project Approval Number: BX20230427), China University of Petroleum (Beijing) Research Initiation Fund (Project Approval Number: 2462023XKBH017).

References

Ahmadi, O., Mortazavi, S.B., Pasdarshahri, H., Mahabadi, H.A., Sarvestani, K., 2019. Modeling of boilover phenomenon consequences: computational fluid dynamics (CFD) and empirical correlations. *Process Saf. Environ. Protect.* 129, 25–39. <https://doi.org/10.1016/j.psep.2019.05.045>.

Apfel, R.E., 1971. Vapor nucleation at a liquid-liquid interface. *J. Chem. Phys.* 54 (1), 62–63. <https://doi.org/10.1063/1.1674639>.

Arai, M., Saito, K., Altenkirch, R.A., 1990. A study of boilover in liquid pool fires supported on water part I: effects of a water sublayer on pool fires. *Combust. Sci. Technol.* 71 (1–3), 25–40. <https://doi.org/10.1080/00102209008951622>.

Blinov, V.I., Khudyakov, G.N., 1961. Diffusion Burning of Liquids. US Army Engineer Research and Development Laboratories. Vicksburg, MS.

Broeckmann, B., Schecker, H.G., 1995. Heat transfer mechanisms and boilover in burning oil-water systems. *J. Loss Prev. Process. Ind.* 8 (3), 137–147. [https://doi.org/10.1016/0950-4230\(95\)00016-T](https://doi.org/10.1016/0950-4230(95)00016-T).

Burgoyne, J.H., 1947. Fires in open tanks of petroleum products: some fundamental aspects. *J. Inst. Petrol.* 33, 158.

Chatris, J.M., Quintela, J., Folch, J., Planas, E., Arnaldos, J., Casal, J., 2001. Experimental study of burning rate in hydrocarbon pool fires. *Combust. Flame* 126 (1–2),

1373–1383. [https://doi.org/10.1016/S0010-2180\(01\)00262-0](https://doi.org/10.1016/S0010-2180(01)00262-0).

Chen, Y.H., Fang, J., Zhang, X.L., Miao, Y.L., Lin, Y.J., Tu, R., Hu, L.H., 2023. Pool fire dynamics: principles, models and recent advances. *Process Saf. Environ. Protect.* 95, 101070. <https://doi.org/10.1016/j.psep.2022.101070>.

Chen, Z., Wei, X.L., 2014. Analysis for combustion properties of crude oil pool fire. *Mech. Eng.* 84, 514–523. <https://doi.org/10.1016/j.proeng.2014.10.463>.

Deng, L., Tang, F., Wang, X.K., 2021. Uncontrollable combustion characteristics of energy storage oil pool: modelling of mass loss rate and flame merging time of annular pools. *Energy* 224, 120181. <https://doi.org/10.1016/j.energy.2021.120181>.

Ditch, B.D., de Ris, J.L., Blanchat, T.K., Chaos, M., Bill, R.G., Dorofeev, S.B., 2013. Pool fires - an empirical correlation. *Combust. Flame* 160 (12), 2964–2974. <https://doi.org/10.1016/j.combustflame.2013.06.020>.

Drysdale, D., 2011. *An Introduction to Fire Dynamics*, third ed. Wiley Blackwell, London.

Ferrero, F., Muñoz, M., Arnaldos, J., 2007a. Effects of thin-layer boilover on flame geometry and dynamics in large hydrocarbon pool fires. *Fuel Process. Technol.* 88 (3), 227–235. <https://doi.org/10.1016/j.fuproc.2006.09.005>.

Ferrero, F., Muñoz, M., Arnaldos, J., 2007b. Thin-layer boilover in diesel-oil fires: determining the increase of thermal hazards and safety distances. *J. Hazard Mater.* 140 (1–2), 361–368. <https://doi.org/10.1016/j.jhazmat.2006.09.062>.

Ferrero, F., Muñoz, M., Kozanoglu, B., Casal, J., Arnaldos, J., 2006. Experimental study of thin-layer boilover in large-scale pool fires. *J. Hazard Mater.* 137 (3), 1293–1302. <https://doi.org/10.1016/j.jhazmat.2006.04.050>.

Garó, J.P., Gillard, P., Vantelon, J.P., Fernandez-Pello, A.C., 1999. Combustion of liquid fuels spilled on water. Prediction of time to start of boilover. *Combust. Sci. Technol.* 147 (1), 39–59. <https://doi.org/10.1080/00102209908924211>.

Garó, J.P., Vantelon, J.P., Fernand-Pello, A.C., 1996. Effect of the fuel boiling point on the boilover burning of liquid fuels spilled on water. *Symp. Combust.* 26 (1), 1461–1467. [https://doi.org/10.1016/S0082-0784\(96\)80367-5](https://doi.org/10.1016/S0082-0784(96)80367-5).

Garó, J.P., Vantelon, J.P., Koseki, H., 2006. Thin-layer boilover: prediction of its onset and intensity. *Combust. Sci. Technol.* 178 (7), 1217–1235. <https://doi.org/10.1080/00102200500296846>.

Hall, H.H., 1925. Oil tank fire boilover. *Mech. Eng.* 47 (7), 540–544.

Hasegawa, K., 1989. Experimental study on the mechanism of hot zone formation in open-tank fires. *Fire Saf. Sci.* 2, 221–230. <https://doi.org/10.3801/IAFSS.FSS.2-221>.

Hottel, H.C., 1959. Certain laws governing the diffusive burning of liquids: a review. *Fire Res. Abstr. Rev.* 1, 41–44.

Hua, J.S., Fan, W.C., Liao, G.X., 1998. Study and prediction of boilover in liquid pool fires with a water sublayer using micro-explosion noise phenomena. *Fire Saf. J.* 30 (3), 269–291. [https://doi.org/10.1016/S0379-7112\(97\)00025-8](https://doi.org/10.1016/S0379-7112(97)00025-8).

Inamura, T., Saito, K., Tagavi, K.A., 1992. A study of boilover in liquid pool fires supported on water. part II: effects of in-depth radiation absorption. *Combust. Sci. Technol.* 86 (1–6), 105–119. <https://doi.org/10.1080/00102209208947190>.

Jarvis, T.J., Donohue, M.D., Katz, J.L., 1975. Bubble nucleation mechanisms of liquid droplets superheated in other liquids. *J. Colloid Interface Sci.* 50 (2), 359–368. [https://doi.org/10.1016/0021-9797\(75\)90240-4](https://doi.org/10.1016/0021-9797(75)90240-4).

Jing, Q., Li, Y.T., Zhang, L.B., Wang, D., Shi, C.L., 2024. Optimization effect of propylene oxide (PO) on evaporation, combustion, and pollutant emissions of high-energy-density JP-10 fuel. *Fuel* 361, 130585. <https://doi.org/10.1016/j.fuel.2023.130585>.

Jing, Q., Wang, D., Shi, C.L., 2023. Effects of aluminum powder additives on deflagration and detonation performance of JP-10/DEE mixed fuel under weak and strong ignition conditions. *Appl. Energy* 331, 120477. <https://doi.org/10.1016/j.apenergy.2022.120477>.

Karataş, A.E., Intasopa, G., Gülder, Ö.L., 2013. Sooting behaviour of n-heptane laminar diffusion flames at high pressures. *Combust. Flame* 160 (9), 1650–1656. <https://doi.org/10.1016/j.combustflame.2013.03.008>.

Kong, D.P., Liu, P.X., Zhang, J.Q., Fan, M.H., Tao, C.F., 2017. Small scale experiment study on the characteristics of boilover. *J. Loss Prev. Process. Ind.* 48, 101–110. <https://doi.org/10.1016/j.jlp.2017.04.008>.

Kong, D.P., Zhao, X.T., Chen, J., Yang, H.B., Du, J., 2021. Study on hazard characteristics and safety distance of small-scale boilover fire. *Int. J. Therm. Sci.* 164, 106888. <https://doi.org/10.1016/j.ijthermalsci.2021.106888>.

Koseki, H., 1993. Boilover and crude oil fire. *J. Appl. Fire Sci.* 3 (3), 243–272. <https://doi.org/10.2190/KGGR-R6X9-KK6L-AXF3>.

Koseki, H., Kokkala, M., Mulholland, G., 1991. Experimental study of boilover in crude oil fires. *Fire Saf. J.* 3, 865–874. <https://doi.org/10.3801/IAFSS.FSS.3-865>.

Koseki, H., Natsume, Y., Iwata, Y., Takahashi, T., Hirano, T., 2006. Large-scale boilover experiments using crude oil. *Fire Saf. J.* 41 (7), 529–535. <https://doi.org/10.1016/j.firesaf.2006.05.008>.

Laboureur, D., Aprin, L., Osmont, A., Buchlin, J.M., Rambaud, P., 2013. Small scale thin-layer boilover experiments: physical understanding and modeling of the water sub-layer boiling and the flame enlargement. *J. Loss Prev. Process. Ind.* 26 (6), 1380–1389. <https://doi.org/10.1016/j.jlp.2013.08.016>.

Li, Y.T., Wu, Z.L., Jing, Q., Zhang, L.B., Wang, D., Liu, Q.M., Qi, S., Xu, H.J., Li, Y.Y., 2024. Optimization effect and reaction mechanism of flake aluminum powder on the combustion performance of high-energy-density JP-10/PO composite fuel. *Combust. Flame* 262, 113369. <https://doi.org/10.1016/j.combustflame.2024.113369>.

Liu, C.X., Ding, L., Jangi, M., Ji, J., Yu, L.X., 2021. Effects of ullage height on heat feedback and combustion emission mechanisms of heptane pool fires. *Fire Saf. J.* 124, 103401. <https://doi.org/10.1016/j.firesaf.2021.103401>.

Nakakuki, A., 1997. Heat transfer in hot-zone-forming pool fires. *Combust. Flame*

- 109 (3), 353–369. [https://doi.org/10.1016/S0010-2180\(96\)00183-6](https://doi.org/10.1016/S0010-2180(96)00183-6).
- Persson, H., Lönnermark, A., 2004. Tank fires-review of fire incidents 1951-2003. SP Swedish National Testing and Research Institute, Borås.
- Ping, P., He, X., Kong, D.P., Wen, R.X., Zhang, Z., Liu, P.X., 2018. An experimental investigation of burning rate and flame tilt of the boilover fire under cross air flows. *Appl. Therm. Eng.* 133, 501–511. <https://doi.org/10.1016/J.APPLTHERMALENG.2018.01.066>.
- Quintiere, J.G., 2006. *Fundamentals of Fire Phenomena*. John Wiley and Sons, London.
- Reed-Hill, R.E., Abbaschian, R., Abbaschian, R., 1973. *Physical Metallurgy Principles*. Van Nostrand, New York.
- Shaluf, I.M., Abdullah, S.A., 2011. Floating roof storage tank boilover. *J. Loss Prev. Process. Ind.* 24 (1), 1–7. <https://doi.org/10.1016/j.jlp.2010.06.007>.
- Tseng, T.Y., Wu, C.L., Tsai, K.C., 2020. Effect of bubble generation on hot zone formation in tank fires. *J. Loss Prev. Process. Ind.* 68, 104314. <https://doi.org/10.1016/j.jlp.2020.104314>.
- Vali, A., Nobes, D.S., Kostiuk, L.W., 2014. Transport phenomena within the liquid phase of a laboratory-scale circular methanol pool fire. *Combust. Flame* 161 (4), 1076–1084. <https://doi.org/10.1016/j.combustflame.2013.09.028>.
- Vali, A., Nobes, D.S., Kostiuk, L.W., 2015. Fluid motion and energy transfer within burning liquid fuel pools of various thicknesses. *Combust. Flame* 162 (4), 1477–1488. <https://doi.org/10.1016/j.combustflame.2014.11.013>.
- Wan Kamarudin, W.N.I., Buang, A., 2016. Small scale boilover and visualization of hot zone. *J. Loss Prev. Process. Ind.* 44, 232–240. <https://doi.org/10.1016/j.jlp.2016.09.018>.
- Zhao, J.L., Huang, H., Jomaas, G., Zhong, M.H., Yang, R., 2018. Experimental study of the burning behaviors of thin-layer pool fires. *Combust. Flame* 193, 327–334. <https://doi.org/10.1016/j.combustflame.2018.03.018>.
- Zhao, J.L., Zhang, X., Song, G.H., Huang, H., Zhang, J.P., 2023. Experiments and modeling of the temperature profile of turbulent diffusion flames with large ullage heights. *Fuel* 331, 125876. <https://doi.org/10.1016/j.fuel.2022.125876>.
- Zhao, J.L., Zhang, X., Zhang, J.P., Wang, W., Chen, C.K., 2022. Experimental study on the flame length and burning behaviors of pool fires with different ullage heights. *Energy* 246, 123397. <https://doi.org/10.1016/j.energy.2022.123397>.
- Zhao, X.R., Al-Abdrabnabi, R., Wu, Y.S., Zhou, X.M., 2021. Evaluations of the feasibility of oil storage in depleted petroleum reservoirs through experimental modelling studies. *Fuel* 294, 120316. <https://doi.org/10.1016/j.fuel.2021.120316>.